Single-Particle Tracking: Effects of Corrals

Michael J. Saxton
Institute of Theoretical Dynamics, University of California, Davis, California 95616, and Laboratory of Chemical Biodynamics, Lawrence Berkeley National Laboratory, University of California, Berkeley, California 94720 USA

ABSTRACT Structural proteins of the membrane skeleton are thought to form "corrals" at the membrane surface, and these corrals may restrict lateral diffusion of membrane proteins. Recent experimental developments in single-particle tracking and laser trapping make it possible to examine the corral model in detail. Techniques to interpret these experiments are presented. First, escape times for a diffusing particle in a corral are obtained from Monte Carlo calculations and analytical solutions for various corral sizes, shapes, and escape probabilities, and reduced to a common curve. Second, the identification of corrals in tracking experiments is considered. The simplest way to identify corrals is by sight. If the walls are impermeable enough, a trajectory fills the corral before the diffusing particle escapes. The fraction of distinct sites visited before escape is calculated for corrals of various sizes, shapes, and escape probabilities, and reduced to a common curve. This fraction is also a measure of the probability that the diffusing species will react with another species in the corral before escaping. Finally, the effect of the sampling interval on the measurement of the short-range diffusion coefficient is examined.

INTRODUCTION

It has long been thought that structural proteins of the membrane skeleton form "corrals" near the membrane surface and that these corrals restrict the lateral diffusion of membrane proteins. The corral model was proposed by Sheetz (1983) and was further developed into the gate model (Tsuji and Ohnishi, 1986; Tsuji et al., 1988). The long-range diffusion coefficient of the gate model is given by a percolation model (Saxton, 1989). The general topic of domains in membranes has been reviewed recently (Edidin, 1992, 1993; Jacobson and Vaz, 1992; Sheetz, 1993; Vaz and Almeida, 1993; Zhang et al., 1993).

Sheetz et al. (1980) clearly demonstrated the effect of the membrane skeleton on lateral diffusion. They measured long-range lateral diffusion rates in normal erythrocytes and spherocytes lacking a membrane skeleton. The diffusion coefficient of the anion transport protein, band 3, was higher by a factor of 50 in the spherocytic cells. Other experiments showed that the diffusion coefficient was increased by treatments that weaken association of membrane skeleton components and was decreased by treatments that strengthen association (Golan and Veatch, 1980; Sheetz, 1983; Tsuji and Ohnishi, 1986; Tsuji et al., 1988).

Two recent experimental developments provide new ways to test the corral model. First, in single-particle tracking experiments, computer-enhanced video microscopy is used to measure the motion of individual proteins on the cell surface (Anderson et al., 1992; de Brabander et al., 1991; Fein et al., 1993; Ghosh, 1991; Ghosh and Webb, 1987, 1994; Hicks and Angelides, 1995; Kucik et al., 1990; Kusumi et al., 1993; Mecham et al., 1991; Schmidt et al., 1993; Sheetz and Elson, 1993; Sheetz et al., 1989; Wang et al., 1994; Zhang et al., 1991). Second, laser traps can be used to move individual proteins across the cell surface with a known force. The motion is again observed by computer-enhanced video microscopy (Edidin et al., 1991; Sako and Kusumi, 1995; Svoboda and Block, 1994).

In single-particle tracking, membrane proteins are labeled with a highly fluorescent label or with colloidal gold microspheres. The trajectories of individual particles are tracked as they move on the cell surface. The time resolution is typically 1/30 s, and the spatial resolution is 5–50 nm. The power of this technique was demonstrated in recent work by Sako and Kusumi (1994) on the transferrin receptor in the plasma membrane of cultured rat kidney cells. The receptor appeared to diffuse within a compartment for a time, then move to an adjacent compartment, diffuse within that compartment for a time, and so on.

Laser tweezers make it possible to move particles over the cell surface in a controlled manner by optical forces (Svoboda and Block, 1994). For a laser trap of given strength, the barrier-free path length can be measured (Edidin et al., 1991), and if the strength of the trap is varied, the distribution of barrier heights can be examined (Sako and Kusumi, 1995).

We assume that the corral walls are fixed potential energy barriers. The probability of crossing a barrier is the same in either direction and is independent of time. In contrast, for the erythrocyte membrane skeleton, the walls are thought to act as transient gates (Tsuji and Ohnishi, 1986; Tsuji et al., 1988). If a tracer crosses a gate, the probability that the gate remains open decays with time, and the probability that a tracer immediately re-enters the corral is enhanced. The model could be extended to include this case. We assume the simplest sort of barrier, a line that a tracer can cross with prescribed probability. We shall see that a more detailed model would be useful, specifying the potential energy function between barrier and tracer.

Received for publication 11 April 1995 and in final form 17 May 1995.
Address reprint requests to Dr. Michael Saxton, Institute of Theoretical Dynamics, University of California, Davis, CA 95616-8618. Tel.: 916-752-6163; Fax: 916-752-7297; E-mail: mjsaxton@ucdavis.edu.

0006-3495/95/08/389/10 $2.00

We calculate the escape time t_{ESC} from a corral and the fraction of distinct sites visited before escape F_{DSVE} as a function of the escape probability P, the corral size a, and the diffusive step size ℓ. The probability that the tracer will react with a species in the corral before escaping is proportional to the fraction F_{DSVE}. This fraction also indicates whether it is possible to identify the corral by sight. If a tracer diffuses in a corral long enough before escaping, its trajectory outlines the corral. We show that a mathematical test for trapping proposed earlier (Saxton, 1993) is a more sensitive test for corrals than identification purely by sight. We also examine a sampling problem for single-particle tracking measurements of motion in a corral. A particle may diffuse a significant fraction of the corral size in the time between observations (Sako and Kusumi, 1994), resulting in underestimates of the short-range diffusion coefficient.

METHODS

Diffusion calculations for lattices are carried out by modifications of methods described earlier (Saxton, 1987). A tracer is placed at a random position in a single corral and carries out a random walk. The corral boundaries are drawn between lines of lattice points, not connecting the lattice points, so that a tracer can cross the corral boundary but cannot diffuse along it. When the tracer tries to cross a corral boundary, a random number is generated, uniformly distributed between 0 and 1. If the random number is less than the prescribed escape probability, the tracer crosses the boundary; otherwise, it remains at its previous position. The escape time and the fraction of distinct sites visited before escape are recorded. Typically 5×10^4 to 1×10^7 trajectories are used.

Monte Carlo calculations for the continuum are carried out as described earlier (Saxton, 1994). Typically 2.5×10^4 to 1×10^5 trajectories are used. When a tracer collides with the corral wall, it tries to cross with the prescribed escape probability, as in the lattice case. If it does not cross, it remains at the point of intersection of its trajectory with the wall. This condition seems appropriate for a system as viscous as a bilayer. To model a gas-phase system with rigid walls, the tracer would be reflected at the wall.

For diffusion on a lattice, the fraction of distinct sites visited before escape was evaluated. The corresponding quantity for continuum diffusion is the Wiener sausage volume, calculated as follows. For each tracer, the entire trajectory is recorded as a sequence of points. For the point Wiener sausage, each trajectory point is surrounded with a circle of prescribed radius, and the area of this set of overlapping circles is found. For the line Wiener sausage, successive trajectory points are connected with straight lines, each point on the lines is surrounded with a circle of prescribed radius, and the area of this set of overlapping circles is found. To find these areas, a set of (typically 10^5) integration points is generated. For each integration point, the distances to the nearest trajectory point and line are calculated. Histograms of these distances are compiled and, from the cumulative histograms of distances, the areas are found as a function of the radius of the circles. Quasi-random integration points are used (Press et al., 1992). These are much more efficient than random integration points, as verified by test calculations on simple shapes. Typically, 5×10^3 to 1×10^4 trajectories are used.

A simpler and faster way to calculate sausage volumes is to record trajectory points on a fine grid, surround each trajectory point with a circle, and mark the grid points inside the circles. At the end of the trajectory, the marked points are counted. Trajectory lines can be treated similarly. We did not use this approach because we wanted to be able to vary the radius of the circles, and the quality of the grid approximation would change considerably with radius. For calculations at fixed radius, this approach may be preferable.

RESULTS

Individual trajectories for continuum diffusion are shown in Fig. 1 for circular corrals with various escape probabilities. The tracer starts at a random position in the corral and carries out a random walk. At each collision with the boundary, the tracer escapes with probability P. The trajectory outlines the corral only at low values of P.

The Monte Carlo results are in dimensionless units of length $r^* = r/\ell$ and time $t^* = t/\tau_J$, where ℓ is the lattice spacing (or the step size in continuum diffusion), and τ_J is the jump time. The diffusion coefficient is $D = D_0 D^*(C)$, where D_0 is the diffusion coefficient in an unobstructed system, and $D^*(C)$ is a dimensionless diffusion coefficient depending on the obstacle concentration. The only obstacles here are the corral walls, so $D^*(C) = 1$ and D_0 is the diffusion coefficient far from the corral walls. The units are related by $\ell^2 = 4D_0\tau_J$, and the dimensionless mean-square displacement is then $\langle r^{*2} \rangle = D^*(C)t^*$. For clarity we retain the asterisks for dimensionless quantities.

Average escape time from a corral

If a particle is diffusing in a corral with semipermeable walls, how long does it take to escape? We can find the escape time analytically or by Monte Carlo calculations, depending on the geometry of the corral. We do not know the shape of the corrals in cells, so it is useful to see how sensitive to shape the escape time is.

The concentration $C(r, t)$ of diffusing particles in a corral is the solution of the diffusion equation

$$\partial C(r, t)/\partial t = D\nabla^2 C(r, t), \quad (1)$$

where the initial condition is a uniform distribution, and the boundary condition is

$$\partial C/\partial r = hC \quad (2)$$

on the corral walls. If $h \to 0$, the wall is perfectly impermeable, and if $h \to \infty$, the wall is perfectly permeable. The

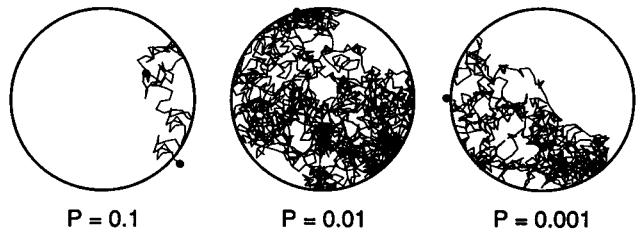

FIGURE 1 Trajectories for continuum diffusion in circular corrals with escape probabilities $P = 0.1$, 0.01, and 0.001. The radius is 10 steps. The initial and final points are shown as filled circles. For the trajectory with $P = 0.1$, there are 18 collisions with the wall in 105 time steps; for $P = 0.01$, 217 collisions in 1881 steps; and for $P = 0.001$, 75 collisions in 864 steps. Note the randomness of the random walks. The escape time for $P = 0.01$ here is twofold greater than the escape time for $P = 0.001$. Readers should consider what they would conclude about the corral size and shape if the boundary were not shown.

concentration is then integrated over r to give the total number of particles $N(t)$, and from this the average escape time t_{ESC} is found (Lee et al., 1987). The solutions for circular and square corrals (see Appendices A and B) are of the form

$$t_{ESC}/\tau = F(ha), \tag{3}$$

where a is the characteristic length of the corral, A is the corral area, $\tau = A/4D$ is the characteristic diffusion time in the corral, and F is a function depending on the shape of the corral. The limits are $t_{ESC}/\tau \propto 1/ha$ as $ha \to 0$ and $t_{ESC}/\tau \to F(\infty)$ as $ha \to \infty$. For diffusion in a circular corral of radius a, Deutch (1980) obtained a very simple expression for the mean escape time,

$$t_{ESC}/\tau = (4 + ha)/2\pi ha. \tag{4}$$

For more complicated geometries, we can obtain the dimensionless escape time t^*_{ESC} from Monte Carlo calculations. A tracer carries out a random walk on a bounded region on a lattice, and when a tracer tries to cross a boundary, it crosses with probability P. So if $P = 0$, the boundary is perfectly impermeable, and if $P = 1$, the boundary is perfectly permeable. In physical units, the escape time is $t_{ESC} = t^*_{ESC}\tau_J$.

Given an observed corral size and escape time, we can use Eq. 3 to obtain a value of h. Unfortunately h, the logarithmic derivative of the concentration at the wall, is not a very useful parameter, particularly in single-particle tracking experiments. We need a relation between h and P. Razi Naqvi et al. (1982) showed that for a one-dimensional Smoluchowski model

$$h = P/\ell(1 - P), \tag{5}$$

and discussed the validity of the Smoluchowski model. We use Eq. 5 because it is the simplest form with the appropriate limits. The factors of P and $1 - P$ are required to give the limits; the factor of ℓ is required on dimensional grounds. This form is supported by the data collapse to be shown.

We must also define the size parameter a for corrals on the lattice. If the tracers diffuse within a hexagonal corral of radius R, in effect they are absorbed as soon as they move outside that region. So the absorbing boundary is a hexagon of radius $R + 1$, and the number of points in this hexagon is $N = 3(R + 1)^2 + 3(R + 1) + 1$. For a triangular corral of side S (see *inset*, Fig. 2), there are $S + 4$ points on an edge of the absorbing boundary, and the number of points in this triangle is $N = (S + 4)(S + 5)/2$. For a square corral of side S, $N = (S + 3)^2$. For a circular corral of radius R on a triangular lattice, the points in a circle of radius $R + 1$ are counted. The area of one triangle in the triangular lattice is $A_{TRI} = (\sqrt{3}/2)\ell^2$, and we define $a = \sqrt{A_{TRI}N}$ and $a^* = a/\ell$, and similarly for the square lattice. For continuum diffusion, we simply take a to be the square root of the corral area. These definitions were chosen to make $\log(t_{ESC}/\tau)$ at $P = 1$ independent of corral size for each corral shape.

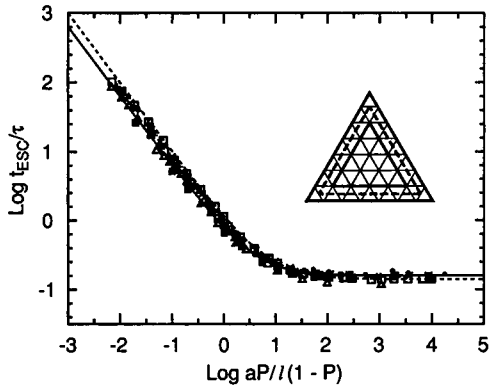

FIGURE 2 Reduced mean escape time t_{ESC}/τ as a function of ha or $aP/\ell(1 - P)$. (——) Analytical results for circular corrals. (- - - -) Analytical results for square corrals. Monte Carlo results for various corral shapes: (△) triangular corral on triangular lattice; (+) hexagonal corral on triangular lattice; (×) circular corral on triangular lattice; (●) circular corral on continuum; (□) square corral on square lattice; (■), square corral on continuum. Escape times for $P = 1$ are not shown. (*inset*) Triangular corral with $S = 4$. The corral boundary (- - - -) is outside the triangle of side 4, and a tracer disappears when it reaches the absorbing boundary, a triangle of side 7 just outside the corral boundary. The number of points in the triangle of side 7 is 36.

With these definitions, the different corral geometries yield similar curves of dimensionless escape time as a function of ha or $aP/\ell(1 - P)$, differing only by a geometrical factor of order one. Results are shown in Fig. 2.

Results for the different corral shapes can be approximated by curves of the form of Eq. 4,

$$t_{ESC}/\tau = (A_1 + A_2x)/x, \tag{6}$$

with $x = ha$ or $x = aP/\ell(1 - P)$, and the parameters given in Table 1. Values of A_2 were obtained from the Monte Carlo results for $P = 1$; values of A_1 were obtained by least-squares fits to the Monte Carlo results for $P < 1$, with the value of A_2 fixed. The "generic" entry is from a two-parameter fit to all of the data points in the figure, 197 Monte Carlo values and 162 analytical values. Values for the generic curve and Eq. 4 differ by at most 15%.

Time and distance scales

To analyze experimental data, what values should we choose for the units of distance ℓ and time τ_J? In unob-

TABLE 1 Parameters for Eq. 6 for various corral shapes

Corral	A_1	A_2
Triangular	0.6291	0.1155 ± 0.0002
Hexagonal	0.8236	0.1536 ± 0.0009
Circular/lattice	0.8290	0.1562 ± 0.0016
Circular/continuum	0.5962	0.1169 ± 0.0097
Circular/analytic	0.6366	0.1592
Square/lattice	0.9132	0.1412 ± 0.0010
Square/continuum	0.5528	0.1548 ± 0.0245
Square/analytic	1.0101	0.1406
Generic	0.7281	0.1516

structed diffusion, there is no problem. Unobstructed diffusion is self-similar, and we can choose any values of ℓ and τ_J related by $\ell^2 = 4D_0\tau_J$. For diffusion in the presence of point obstacles, we take ℓ to be the sum of the tracer radius and the obstacle radius, and we find τ_J from ℓ. For diffusion in corrals, we choose τ_J to be the experimental sampling time, typically 1/30 s, and we find ℓ from τ_J.

Equation 5 shows that an experimental value of h does not determine P uniquely. We must specify a value of ℓ. Thus, P is a function of τ_J, that is, a probability of escape in one jump time. The probability of escape is simply the reciprocal of the average number of collisions required to cross the barrier, so P must depend on the definition of a collision with the barrier.

If we take $\tau_J = 1/30$ s, ℓ may be large enough that a tracer encounters the barrier independently several times between observations. A Brownian bridge treatment can be used to examine this possibility, as in chemical kinetics simulations (Clifford and Green, 1986). Another option would be to choose ℓ to be the barrier width, by analogy with the case of point obstacles. Theoretical arguments suggest that ℓ should be taken to be the velocity correlation length ℓ_V (Calef and Deutch, 1983; Axelrod and Wang, 1994). If the mass of a tracer is m and the temperature is T, the average thermal velocity is $V_{TH} = \sqrt{kT/m}$. The velocity correlation length is $\ell_V = D/V_{TH}$, and the velocity correlation time is $\tau_V = D/V_{TH}^2$. So in a time τ_V, a tracer with velocity V_{TH} travels a distance ℓ_V. The value of h is V_{TH}/D. For a 30-kDa protein at 300 K, $V_{TH} = 9.1$ m/s. For a diffusion coefficient $D_0 = 0.1$ μm^2/s, then, $\tau_V = 1.2$ fs and $\ell_V = 11$ fm. If ℓ is so small, P must also be very small to give the observed value of h. What this means physically is that every collision with the solvent that moves the tracer in the direction of the barrier is counted as an attempt to cross the barrier, so the probability of success must be small.

To treat this problem in more detail, one would need to assume some form for the potential energy of a tracer crossing the barrier, and do, say, a Brownian dynamics calculation of the barrier crossing rate (McCammon et al., 1987). This assumption introduces a molecular length into the problem, the barrier width, and allows a collision to be defined unambiguously. In a Brownian dynamics calculation, a variable time increment would be used, large away from the barrier and small enough near the barrier that the force is approximately constant in one time step. These calculations would yield the probability of crossing per unit time, the crossing times for those tracers that cross, and the return times for those that do not.

Distribution of escape times

We can obtain the distribution of escape times from the Monte Carlo calculations. Typical distributions are shown in Fig. 3. The most probable value is close to the mean value. Peak heights shift somewhat from curve to curve, but the shapes and widths are similar. The distributions are broad, with a full width at half-maximum around 1 to 1½ orders of magnitude. So if an experimental treatment of the corral walls changes P by a factor of 3, one would need to look at many tracers to see an effect. Even with a difference of a factor of 10, there is significant overlap.

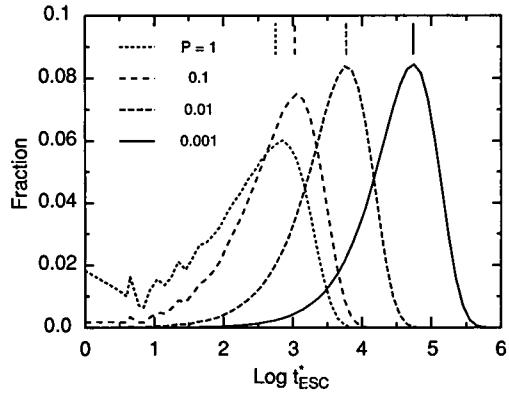

FIGURE 3 Distribution of escape times for diffusion in a hexagonal corral of radius 36, for P = 1, 0.1, 0.01, and 0.001. The vertical lines indicate mean values. The corresponding distributions for continuum diffusion in a circular corral of radius 20 are practically the same shape, but shifted to lower t^*_{ESC} by a factor of 2.65.

Fraction of distinct sites visited before escape

The fraction of distinct sites visited before escape, F_{DSVE}, is a measure of the probability that the diffusing species will react with another species in the corral before leaving the corral, and a measure of the visibility of the corral in a tracking experiment. If the corral walls are impermeable enough, the trajectory of the tracer will outline the corral. But this method of detection has two limitations. First, motion that looks like trapping can occur by chance in an unobstructed random walk. Second, we do not know a priori the size, shape, or position of the corral, or the permeability of the walls.

It is trivial to obtain F_{DSVE} from the Monte Carlo calculations on a lattice; the problem is to reduce the results for various corral sizes, shapes, and escape probabilities to a common curve.

For a simpler problem, the mean-field or well-mixed case, there is an analytical expression for the mean time to visit every site (Nemirovsky and Coutinho-Filho, 1991; Brummelhuis and Hilhorst, 1992). Here a tracer carries out a random walk on a lattice of N sites in which each site is connected to every other site. The mean time to visit every site is in dimensionless units

$$t^*_{MF} = N \sum_{k=1}^{N} \frac{1}{k}, \tag{7}$$

so that in physical units $t_{MF} = t^*_{MF}\tau_J$. In terms of the psi or digamma function (Abramowitz and Stegun, 1972),

$$t^*_{MF} = N[\psi(N+1) - \psi(1)] \sim N \ln N. \tag{8}$$

This sum approaches its asymptotic value very slowly, so we use the exact sum instead of the asymptotic value. (This random-walk problem is asymptotically identical to a standard problem in combinatorics, the coupon collector problem (Feller, 1968), and Eq. 7 is derived there.)

If F_{DSVE} is plotted as a function of $\log t^*_{ESC}$ for various corral sizes, shapes, and escape probabilities, the data are very scattered. But if F_{DSVE} is plotted as a function of $x = t^*_{ESC}/t^*_{MF}$, the points fall on a common curve, as shown in Fig. 4 *a*. Similar plots using quantities other than t^*_{MF}, such as $N \ln N$ or the time to visit all sites (Nemirovsky et al., 1990; Brummelhuis and Hilhorst, 1992), gave worse agreement. As Fig. 4 *a* shows, the data can be approximated by a simple empirical expression

$$F_{DSVE} = x^\alpha/(x_0^\alpha + x^\alpha), \quad (9)$$

where x_0 and α are constants. Here $x_0 = 0.4080$ and $\alpha = 0.9001$.

Fig. 4 *b* shows the distribution of F_{DSVE} for individual random walks in a hexagonal corral of radius 36. As P decreases from 1 to 0.001, the distribution shifts from $\langle F_{DSVE}\rangle = 0.054$ to $\langle F_{DSVE}\rangle = 0.802$. The distributions are broad; the distribution for $P = 0.01$ covers most of the range of F_{DSVE}. Unless P is very small, a tracer does not necessarily visit the entire corral area, and one should consider the area observed to be a lower limit for the corral area, not the corral area. In the experiments of Sako and Kusumi (1994), however, trapped motion in several adjacent corrals was observed, giving a much better measure of the corral size.

Note that t_{MF} is not very sensitive to the value of ℓ. The number of points N in a corral is the ratio of the area of the corral to the area of a lattice triangle, so $N \sim 1/\ell^2$. From Eq. 8, $t^*_{MF} \sim N \ln N \sim (1/\ell^2)\ln(1/\ell^2)$. And, $\tau_J = \ell^2/4D_0$, so $t_{MF} = t^*_{MF}\tau_J \sim \ln(1/\ell^2)$. So we cannot use observed values of F_{DSVE} to determine ℓ.

These results describe diffusion on a lattice. The corresponding results for continuum diffusion are known as the Wiener sausage problem, because the area of an irregular sausage-shaped region surrounding a Wiener process is measured. The Wiener process is the limit of a random walk as the step size goes to zero and is therefore discontinuous at every point. To construct the sausage we draw a circle of prescribed radius at every point on the Wiener process, take the union of the set of points within these circles, and find the area of the union (Mandelbrot, 1983). For an unrestricted random walk in two dimensions, the volume of the Wiener sausage is proportional to the number of distinct sites visited (Berezhkovskii et al., 1989).

In the Monte Carlo calculations, we approximate this as point and line Wiener sausages. To find the point Wiener sausage, we record the position of the tracer at every observed time step, surround each position with a circle of fixed radius, and find the area of the set of overlapping circles. To find the line Wiener sausage, we connect successive trajectory points with straight lines, surround each point on those lines with a circle of fixed radius, and find the area of the set of overlapping circles. The sausages for one random walk are shown in Fig. 5. These approximations are also appropriate in a tracking experiment, where the position of the diffusing particle is measured periodically, not continuously.

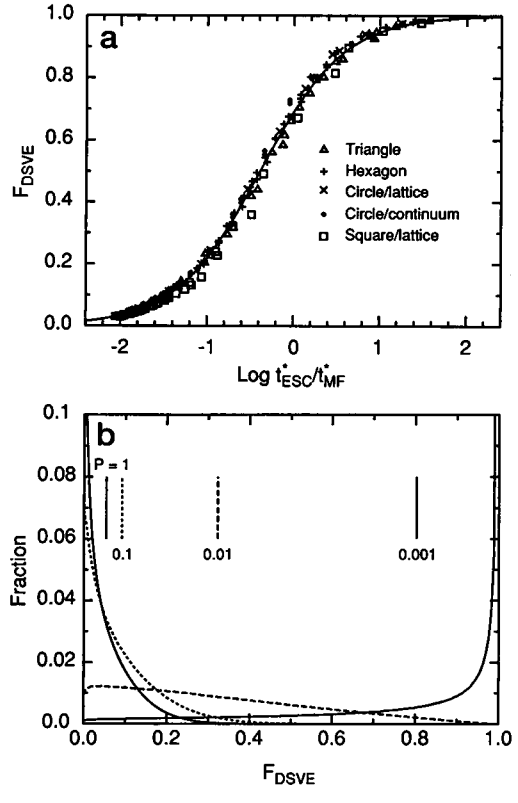

FIGURE 4 (*a*) F_{DSVE} as a function of $\log t^*_{ESC}/t^*_{MF}$ for various corral sizes, shapes, and escape probabilities. For continuum diffusion, calculations were done for $F_{DSVE} \le 0.74$. (——) Equation 9 with $x_0 = 0.4080$ and $\alpha = 0.9001$, obtained by a least-squares fit to the data in *a*. (*b*) Histogram of F_{DSVE} for individual random walks on the triangular lattice in a hexagonal corral of radius 36 for the indicated values of P. The vertical lines show $\langle F_{DSVE}\rangle$.

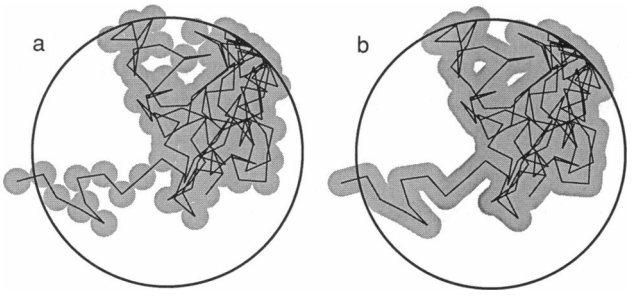

FIGURE 5 Wiener sausage areas for one random walk. (*a*) Point Wiener sausage. (*b*) Line Wiener sausage. The corral radius is 5ℓ, the escape probability is $P = 0.001$, and this random walk is 147 time steps long. This walk does not fill the entire area and would lead to a serious underestimate of the corral area. As Fig. 4 *b* shows, this underestimate is not a fluke, but a normal feature of random walks. Again, readers should consider how they would interpret this random walk if it were observed on a cell surface.

Values of F_{DSVE} from both point and line Wiener sausages are included in Fig. 4 *a* and fall on the common curve, so F_{DSVE} is meaningful for both lattice and continuum diffusion. Values of F_{DSVE} for line Wiener sausages are ~1–7% larger than the values for points. The radius of the circles was chosen to be $\ell/2$ to correspond to the distinct sites visited in a lattice. To use this approach to examine the probability of reaction, the radius would be chosen to be the sum of the radii of the reacting species.

What is the probability that a random walk will stay within a bounded region?

Earlier work discussed the probability $\Psi(R,t)$ that an unobstructed random walk starting at the origin at $t = 0$ remains within a region of radius R for all times $\leq t$ (Saxton, 1993). The family of curves for different R can be reduced to a single curve by plotting Ψ as a function of Dt/R^2 (in physical units, not dimensionless units). For $Dt/R^2 > 0.1$, this curve is a straight line

$$\log \Psi = 0.2048 - 2.5117(Dt/R^2). \quad (10)$$

This expression can be used to test the reality of what appear to be corrals.

Equation 10 is a more sensitive test than simply looking for corrals. Table 2 shows values for Ψ and F_{DSVE} for point Wiener sausages for continuum diffusion in a circular corral of radius 20. We assume that the tracer starts at the center of the corral at $t = 0$, so that $R = 20$, and we assume $t = t_{ESC}$. Values of Ψ are calculated from Eq. 10; for $P \geq 0.5$, the exact values are 2.0–2.5% lower (Saxton, 1993, Eq. A3). For $P = 0.01$, only 35% of the sites are visited, so the corral is not fully outlined by the trajectory, but the value of Ψ is small enough to indicate unequivocally the presence of a corral. But corrals with more permeable walls are not particularly obvious in either test. For $P = 0.1$, only 10% of the sites are visited, and the probability is almost 40% that such a trajectory would occur in an unobstructed random walk. But the escape time is increased 1.8-fold over the value for free diffusion. So there could be a network of moderately permeable barriers not readily detected by tracking experiments, but sufficient to slow long-range lateral diffusion by a factor of two or so. Presumably such barriers could be detected by laser tweezer experiments.

TABLE 2 Tests for presence of a corral

P	t^*_{ESC}	Ψ	F_{DSVE}
0.01	2226.4	0.00051	0.350
0.02	1214.3	0.0199	0.234
0.05	609.0	0.177	0.141
0.10	394.4	0.385	0.100
0.20	296.4	0.549	0.0797
0.50	231.1	0.695	0.0654
0.75	223.1	0.715	0.0635
1.00	214.1	0.739	0.0612

Interpretation of experimental data

Sako and Kusumi (1994) found an average compartment radius $a = 0.28$ μm, an average escape time $t_{ESC} = 29$ s, and a short-range diffusion coefficient $D_0 = 0.1$ μm²/s. These results clearly indicate corralling. Simply from the relation $\langle r^2 \rangle = 4\,Dt$, the root-mean-square displacement for a freely diffusing particle is 3.4 μm in 29 s, suggesting confinement. More quantitatively, assume that the tracer starts at one edge of the corral and diffuses to the other edge, so that $R = 2a$. Then, from Eq. 10, the probability of a displacement no larger than R in a random walk by a free particle is 9×10^{-24}.

Next, we find P and F_{DSVE}, assuming for simplicity a circular corral. The characteristic time for diffusion in the corral is $\tau = \pi a^2/4D_0 = 0.616$ s, and $t_{ESC} = 29$ s, so $t_{ESC}/\tau = 47.1$. Then from Eq. 4, $h = 0.0485\ \mu m^{-1}$. If we take the jump time τ_J to be 1/30 s, then $\ell = \sqrt{4D_0\tau_J} = 0.116$ μm, and from Eq. 5, $P = 5.57 \times 10^{-3}$. The corral area $A_{COR} = 0.246$ μm², and the area of a triangle in the triangular lattice is $A_{TRI} = (\sqrt{3}/4)\ell^2 = 0.00578$ μm². So the number of points in the corral is $N = A_{COR}/A_{TRI} = 42.6$. From Eq. 7, by interpolation, $t^*_{MF} = 185$, so $t_{MF} = t^*_{MF}\tau_J = 6.17$ s. From Eq. 9, then, $F_{DSVE} = 0.90$.

Suppose that the sampling time is 1/3 s as in Fig. 2 of Sako and Kusumi (1994). Similar calculations with $\tau_J = 1/3$ s instead of 1/30 s show that P increases by a factor of $\approx \sqrt{10}$ to 0.0174, and $F_{DSVE} = 0.94$, a plausible value.

Suppose we choose ℓ to be a typical lipid dimension, 0.8 nm. Then $P = 3.88 \times 10^{-5}$, and $F_{DSVE} = 0.756$. So P is sensitive to the choice of ℓ because P is a function of τ_J, but the value of F_{DSVE} is not very sensitive to ℓ, as pointed out earlier.

Short-range diffusion coefficients: the effect of the sampling rate

In measuring short-range diffusion coefficients, a problem arises because a tracer may diffuse a significant fraction of the corral size in the time between successive measurements of its position (Sako and Kusumi, 1994). For a domain radius of 0.28 μm and a sampling time of 33.3 ms, a freely diffusing tracer with diffusion coefficient $D_0 = 1$ μm²/s would diffuse on average 0.37 μm, 130% of the corral radius. A protein with $D_0 = 0.1$ μm²/s, as observed by Sako and Kusumi (1994), would diffuse 0.12 μm between measurements, ~40% of the corral radius, and a protein with $D_0 = 0.01$ μm²/s would diffuse 0.037 μm, ~13% of the corral radius.

The problem that will arise is shown in the inset to Fig. 6. Suppose that a tracer near the boundary hits the boundary between observations. Its actual path is *ABC*, but the path attributed to it is *AC*, so the mean-square displacement and the diffusion coefficient are underestimated. Of course, in free diffusion, a tracer could follow a similar path, but the probability of such a path is changed when barriers are present.

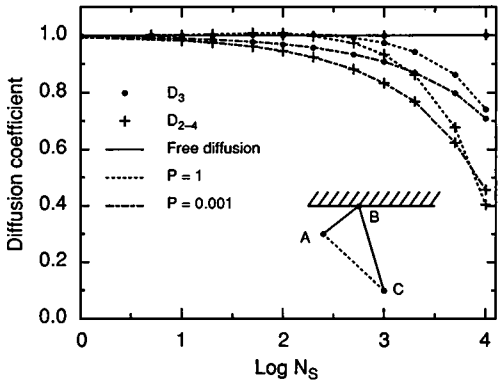

FIGURE 6 Values of the short-range diffusion coefficients D_3 (Eq. 12b) and D_{2-4} (Eq. 12d) for various sampling intervals. Continuum Monte Carlo calculations were carried out for free diffusion and for diffusion in a circle of radius 200 step sizes, and escape probabilities $P = 0.1$ and 0.001. Positions were recorded every N_S time steps, mean-square displacements were calculated for these positions, and the diffusion coefficients found. For free diffusion, the sampling interval has no effect; for confined diffusion, the sampling interval may lower the short-range diffusion coefficient significantly. (*inset*) See text.

We examine this problem by Monte Carlo calculations. A tracer carries out a random walk with a step size much less than the corral size. The position resulting from this underlying random walk is sampled every N_S time steps, and the mean-square displacement is obtained from the sampled random walk. The short-term diffusion coefficient of the underlying random walk is 1, and we evaluate the short-term diffusion coefficient for the sampled random walk.

The short-term diffusion coefficient of the sampled random walk is obtained from the mean-square displacement over a few sampling times. For example, Sako and Kusumi (1994) use D_{2-4}, obtained by plotting the mean-square displacement as a function of time for $\Delta t = 2$, 3, and 4, and finding the slope of this line. Because so few time points are used, it is useful to do the least-squares fit analytically and obtain an expression for D in terms of the observed mean-square displacements (MSD) $\langle r^2(n)\rangle$. If all points are weighted equally, the slope of a least-squares line is

$$D = (NS_{XY} - S_X S_Y)/(NS_{XX} - S_X^2), \tag{11}$$

where N is the number of points, $S_X = \sum_{i=1}^{N} X_i$, and so forth. We assume that $\langle r^2(0)\rangle = 0$ is a data point, and obtain

$$D_2 = [\langle r^2(1)\rangle - \langle r^2(0)\rangle]/1, \tag{12a}$$

$$D_3 = [\langle r^2(2)\rangle - \langle r^2(0)\rangle]/2, \tag{12b}$$

$$D_4 = [-3\langle r^2(0)\rangle - \langle r^2(1)\rangle + \langle r^2(2)\rangle + 3\langle r^2(3)\rangle]/10, \tag{12c}$$

$$D_{2-4} = [\langle r^2(4)\rangle - \langle r^2(2)\rangle]/2. \tag{12d}$$

Note that some of the MSDs cancel out.

For an unconfined random walk, the distribution of independent MSDs is a gamma distribution depending on the number of measurements K (Qian et al., 1991). In the limit of large K, the gamma distribution yields a Gaussian distribution. For a confined random walk, however, the distributions of MSDs are shifted, leading to a shift in the diffusion coefficients.

Values of the diffusion coefficients D_3 and D_{2-4} are shown in Fig. 6 as a function of the sampling interval N_S. For free diffusion, $D = 1$ for all definitions of D and all sampling intervals, as expected. The sampling procedure simply rescales time by a factor N_S and rescales distance by a factor $\sqrt{N_S}$, leaving D unchanged. For confined diffusion, the observed diffusion coefficient can be 1/2 to 2/3 of the true value, depending on the sampling interval and the definition of D. The error increases as the number of time steps included in the MSDs increases. The error decreases as the corral size increases.

Two approaches can be used to see whether this problem arises in experimental data. First, one can calculate short-term Ds using several definitions and see how well they agree. Second, one can identify the boundary and calculate the Ds using only that part of the trajectory at least one step size away from the boundary.

DISCUSSION

We have shown that the escape time for corrals of different sizes, shapes, and escape probabilities can be reduced to a common curve by plotting a reduced escape time t_{ESC}/τ as a function of ha for analytical results, and $aP/\ell(1 - P)$ for Monte Carlo results, where a is the corral size, ℓ is the length of a diffusion step and P is the probability of escape in one jump time τ_J. The dependence on shape is weak, at least for the compact shapes considered, so that the simple formulas Eqs. 4 or 6 can be used as a first approximation.

The distribution of escape times from a corral is broad, at least an order of magnitude wide. One must be cautious, then, in interpreting experimental results on a few diffusing particles. If an experimental treatment to strengthen or weaken the corral walls changed the escape probability by, say, a factor of three, it would be necessary to look at the effects on many diffusing particles to establish that there is an effect.

The fraction of distinct sites visited before escape, F_{DSVE}, is a measure of the visibility of the corral in a tracking experiment, and the probability of reaction before escape. Values of F_{DSVE} for corrals of various sizes, shapes, and escape probabilities can be reduced to a common curve by plotting them as a function of the ratio of the escape time t_{ESC} to the time t_{MF} to visit all sites in a well-mixed corral of the same size. The distribution of F_{DSVE} for individual random walks is broad, so that the size obtained by looking at a trajectory should be viewed as a lower limit.

For confined diffusion, the finite sampling rate implies that collisions of a tracer with the boundary may occur between observations, reducing the observed short-range diffusion coefficient. To test for this problem, one can compare various short-range Ds and calculate the Ds using only that part of the trajectory at least one step size away from the boundary.

To understand the escape probability, we need to consider the mechanism of escape, as discussed by Bashford (1986). We have assumed that the walls are static potential energy barriers. Each attempt to cross the barrier is independent, and the probability of immediately recrossing a barrier is the same as the probability of crossing it in the first place. Note that in this model an isolated corral would be visible both because it would confine internal particles and because it would exclude external particles.

Another possibility is that the walls are fluctuating gates, with some characteristic fluctuation time (Bashford, 1986). If the gates open and close much faster than the average time between attempts to cross the boundary, the situation is the same as for static barriers. If the gates open and close at a rate slower than the time between attempts to cross the boundary, then attempts to cross are correlated. If a tracer crosses the boundary, the gate is open and there is a higher probability that the gate will remain open and the tracer will recross in the opposite direction. This process could easily be incorporated into the model.

What happens in erythrocytes? In the idealized membrane skeleton, the corrals are equilateral triangles of side 76 nm and the diffusion coefficient in the absence of corrals is the value for spherocytes, $D = 0.25\ \mu m^2/s$ (Sheetz et al., 1980), so the characteristic time for diffusion is 5.8 ms. The characteristic time for spectrin-spectrin association in the erythrocyte is not known. The value in bulk solution is 625 s (Ungewickell and Gratzer, 1978), but the actual value in the cell may be less, on account of the high concentration of spectrin at the membrane and the presence of compounds affecting association. An estimate based on the bond percolation model suggests a value ~0.1 s (Saxton, 1989). In either case, diffusion is fast compared with the association time.

Laser trap experiments could clarify the situation. If one tried to move a protein across a barrier repeatedly at the same point, one could see if the probability changed with time. If there were gate-opening and gate-closing events, one could obtain a rough bound on the rate, at least good enough to distinguish 625 s from 0.1 s.

I thank K. Jacobson, A. Kusumi, E. D. Sheets, and R. Simson for helpful discussions.

This work was supported by National Institutes of Health grant GM38133.

APPENDIX A

Escape time from circle

The diffusion equation is

$$\frac{\partial C(r,t)}{\partial t} = \frac{D}{r}\frac{\partial}{\partial r}\left[r\frac{\partial C(r,t)}{\partial r}\right], \tag{A1}$$

where $C(r,t)$ is the concentration of diffusing particles and D is the diffusion coefficient. The initial condition is a uniform distribution, and the boundary condition is

$$\partial C/\partial r = hC \tag{A2}$$

at $r = R$. The concentration of diffusing particles at position r and time t due to a cylindrical source at position r' at $t = 0$ is (Carslaw and Jaeger, 1959, p. 369)

$$C(r, r', t) = \left[\frac{1}{\pi a^2}\right]^2 \sum_{n=1}^{\infty} \frac{J_0(\alpha_n r)J_0(\alpha_n r')}{J_0^2(\alpha_n a) + J_1^2(\alpha_n a)} \exp(-\alpha_n^2 Dt), \tag{A3}$$

where J_0 and J_1 are Bessel functions, and the α_n are the positive roots of

$$haJ_0(\alpha a) - \alpha a J_1(\alpha a) = 0. \tag{A4}$$

If we assume a uniform initial distribution, the total number of particles $N(t)$ in the corral is obtained by integrating over r and r', using (Gradshteyn and Ryzhik, 1994)

$$\int_0^a 2\pi r dr J_0(\alpha r) = (2\pi a/\alpha)J_1(\alpha a) \tag{A5}$$

to give

$$N(t) = 4\sum_{n=1}^{\infty} \frac{1}{(\alpha_n a)^2} \frac{J_1^2(\alpha_n a)}{J_0^2(\alpha_n a) + J_1^2(\alpha_n a)} \exp(-\alpha_n^2 Dt). \tag{A6}$$

But (Lee et al., 1987)

$$t_{ESC} = \int_0^{\infty} N(t)dt, \tag{A7}$$

so that

$$t_{ESC}/\tau = \frac{16}{\pi}\sum_{n=1}^{\infty} \frac{1}{(\alpha_n a)^4} \frac{J_1^2(\alpha_n a)}{J_0^2(\alpha_n a) + J_1^2(\alpha_n a)}, \tag{A8}$$

where $\tau = \pi a^2/4D$. In the limit as $ha \to 0$, $t_{ESC}/\tau \to 2/\pi ha$, and in the limit as $ha \to \infty$, $t_{ESC}/\tau \to 1/2\pi$; the required sum over the roots of the Bessel function is evaluated by Davis (1962).

APPENDIX B

Escape time from square

The escape time from a square corral is obtained similarly. From Carslaw and Jaeger (1959, pp. 33–34 and 360–361) the two-dimensional Green's function is the product of two one-dimensional functions:

$$C(x, y, x', y', t) =$$

$$\sum_{m,n=1}^{\infty} Z_m(x)Z_n(x')Z_m(y)Z_n(y')\exp[-D(\alpha_m^2 + \alpha_n^2)t], \tag{B1}$$

where

$$Z_m(x) = A_m^{1/2}[\alpha_m \cos(\alpha_m x) + h \sin(\alpha_m x)], \tag{B2}$$

$$A_m = 2a/[(\alpha_m a)^2 + (ha)^2 + 2ha], \tag{B3}$$

and the α_m are defined by

$$\tan(\alpha a) = 2\alpha h/(\alpha^2 - h^2). \tag{B4}$$

Then the total number of particles in the corral is

$$N(t) = \frac{1}{a^2}\int_0^a\int_0^a\int_0^a\int_0^a dxdydx'dy'C(x, y, x', y', t) \quad \text{(B5)}$$

We do the integrals and use Eq. B4 to simplify the result, obtaining

$$N(t) = \frac{1}{a^2}\sum_{m,n=1}^{\infty} I_m^2 I_n^2 \exp[-D(\alpha_m^2 + \alpha_n^2)t], \quad \text{(B6)}$$

and on integrating over t, we obtain

$$t_{ESC}/\tau = \frac{4}{a^2}\sum_{m,n=1}^{\infty} I_m^2 I_n^2 \frac{1}{(\alpha_m a)^2 + (\alpha_n a)^2}, \quad \text{(B7)}$$

where

$$\tau = a^2/4D \quad \text{(B8)}$$

and

$$I_m = A_m^{1/2}\frac{ha}{\alpha_m a}\left[\frac{(\alpha_m a)^2 + (ha)^2}{(\alpha_m a)^2 - (ha)^2}\cos(\alpha_m a) + 1\right]. \quad \text{(B9)}$$

In the limit as $ha \to 0$, $t_{ESC}/\tau \to 1/ha$, and in the limit as $ha \to \infty$,

$$t_{ESC}/\tau \to \frac{256}{\pi^6}\sum_{\substack{m,n=1\\ m,n \text{ odd}}}^{\infty}\frac{1}{m^2n^2}\frac{1}{m^2 + n^2} = 0.140577. \quad \text{(B10)}$$

REFERENCES

Abramowitz, M., and I. A. Stegun. 1972. Handbook of Mathematical Functions. U. S. Government Printing Office, Washington, D.C. 258.

Anderson, C. M., G. N. Georgiou, I. E. G. Morrison, G. V. W. Stevenson, and R. J. Cherry. 1992. Tracking of cell surface receptors by fluorescence digital imaging microscopy using a charge-coupled device camera. Low-density lipoprotein and influenza virus receptor mobility at 4°C. *J. Cell Sci.* 101:415–425.

Axelrod, D., and M. D. Wang. 1994. Reduction-of-dimensionality kinetics at reaction-limited cell surface receptors. *Biophys. J.* 66:588–600.

Bashford, D. 1986. Fluctuation and rotation in diffusion-influenced monomolecular reactions. *J. Chem. Phys.* 85:6999–7010.

Berezhkovskii, A. M., Yu. A. Makhnovskii, and R. A. Suris. 1989. Wiener sausage volume moments. *J. Stat. Phys.* 57:333–346.

Brummelhuis, M. J. A. M., and H. J. Hilhorst. 1992. How a random walk covers a finite lattice. *Physica A.* 185:35–44.

Calef, D. F., and J. M. Deutch. 1983. Diffusion-controlled reactions. *Annu. Rev. Phys. Chem.* 34:493–524.

Carslaw, H. S., and J. C. Jaeger. 1959. Conduction of Heat in Solids, 2nd ed. Clarendon Press, Oxford. 510 pp.

Clifford, P., and N. J. B. Green. 1986. On the simulation of the Smoluchowski boundary condition and the interpolation of brownian paths. *Mol. Phys.* 57:123–128.

Davis, H. T. 1962. The Summation of Series. The Principia Press of Trinity University, San Antonio, TX. p. 111.

de Brabander, M., R. Nuydens, A. Ishihara, B. Holifield, K. Jacobson, and H. Geerts. 1991. Lateral diffusion and retrograde movements of individual cell surface components on single motile cells observed with Nanovid microscopy. *J. Cell Biol.* 112:111–124.

Deutch, J. M. 1980. A simple method for determining the mean passage time for diffusion controlled processes. *J. Chem. Phys.* 73:4700–4701.

Edidin, M. 1992. Patches, posts and fences: proteins and plasma membrane domains. *Trends Cell Biol.* 2:376–380.

Edidin, M. 1993. Patches and fences: probing for plasma membrane domains. *J. Cell Sci. Suppl.* 17:165–169.

Edidin, M., S. C. Kuo, and M. P. Sheetz. 1991. Lateral movements of membrane glycoproteins restricted by dynamic cytoplasmic barriers. *Science.* 254:1379–1382.

Fein, M., J. Unkeless, F. Y. S. Chuang, M. Sassaroli, R. da Costa, H. Väänänen, and J. Eisinger. 1993. Lateral mobility of lipid analogues and GPI-anchored proteins in supported bilayers determined by fluorescent bead tracking. *J. Membr. Biol.* 135:83–92.

Feller, W. 1968. An Introduction to Probability Theory and Its Applications, Vol. I, 3rd ed. John Wiley & Sons, New York. 224–225.

Ghosh, R. N. 1991. Mobility and clustering of individual low-density lipoprotein receptor molecules on the surface of human skin fibroblasts. Ph.D. thesis. Cornell University, Ithaca, NY. 260 pp.

Ghosh, R. N., and W. W. Webb. 1987. Low density lipoprotein (LDL) receptor dynamics on cell surfaces. *Biophys. J.* 51:520*a*. (Abstr.)

Ghosh, R. N., and W. W. Webb. 1994. Automated detection and tracking of individual and clustered cell surface low density lipoprotein receptor molecules. *Biophys. J.* 66:1301–1318.

Golan, D. E., and W. Veatch. 1980. Lateral mobility of band 3 in the human erythrocyte membrane studied by fluorescence photobleaching recovery: evidence for control by cytoskeletal interactions. *Proc. Natl. Acad. Sci. USA.* 77:2537–2541.

Gradshteyn, I. S., and I. M. Ryzhik. 1994. Table of Integrals, Series, and Products, 5th ed. Academic Press, Boston, MA. 707 pp.

Hicks, B. W., and K. J. Angelides. 1995. Tracking movements of lipids and Thy1 molecules in the plasmalemma of living fibroblasts by fluorescence video microscopy with nanometer scale precision. *J. Membr. Biol.* 144:231–244.

Jacobson, K., and W. L. C. Vaz, editors. 1992. Domains in biological membranes. *Comments Mol. Cell. Biophys.* 8:1–114.

Kucik, D. F., E. L. Elson, and M. P. Sheetz. 1990. Cell migration does not produce membrane flow. *J. Cell Biol.* 111:1617–1622.

Kusumi, A., Y. Sako, and M. Yamamoto, 1993. Confined lateral diffusion of membrane receptors as studied by single particle tracking (Nanovid microscopy). Effects of calcium-induced differentiation in cultured epithelial cells. *Biophys. J.* 65:2021–2040.

Lee, S. Y., M. Karplus, D. Bashford, and D. Weaver. 1987. Brownian dynamics simulation of protein folding: a study of the diffusion-collision model. *Biopolymers.* 26:481–506.

Mandelbrot, B. B. 1983. The Fractal Geometry of Nature. W. H. Freeman and Co., New York. p. 32.

McCammon, J. A., R. J. Bacquet, S. A. Allison, and S. H. Northrup. 1987. Trajectory simulation studies of diffusion-controlled reactions. *Faraday Discuss. Chem. Soc.* 83:213–222.

Mecham, R. P., L. Whitehouse, M. Hay, A. Hinek, and M. P. Sheetz. 1991. Ligand affinity of the 67-kD elastin/laminin binding protein is modulated by the protein's lectin domain: visualization of elastin/laminin-receptor complexes with gold-tagged ligands. *J. Cell Biol.* 113:187–194.

Nemirovsky, A. M., and M. D. Coutinho-Filho. 1991. Lattice covering time in D dimensions: theory and mean field approximation. *Physica A.* 177:233–240.

Nemirovsky, A. M., H. O. Martin, and M. D. Coutinho-Filho. 1990. Universality in the lattice-covering time problem. *Phys. Rev. A.* 41: 761–767.

Press, W. H., S. A. Teukolsky, W. T. Vetterling, and B. P. Flannery. 1992. Numerical Recipes in FORTRAN: The Art of Scientific Computing, 2nd ed. Cambridge University Press, Cambridge. 299–305.

Qian, H., M. P. Sheetz, and E. L. Elson. 1991. Single particle tracking. Analysis of diffusion and flow in two-dimensional systems. *Biophys. J.* 60:910–921.

Razi Naqvi, K., K. J. Mork, and S. Waldenstrøm. 1982. On describing the steady absorption of Brownian particles by a restricted random walk. *Chem. Phys. Lett.* 92:156–159.

Sako, Y., and A. Kusumi. 1994. Compartmentalized structure of the plasma membrane for receptor movements as revealed by a nanometer-level motion analysis. *J. Cell Biol.* 125:1251–1264.

Sako, Y., and A. Kusumi. 1995. Barriers for lateral diffusion of transferrin receptors in the plasma membrane as characterized by receptor dragging by laser tweezers: fence versus tether. *J. Cell Biol.* 129:1559–1574.

Saxton, M. J. 1987. Lateral diffusion in an archipelago: the effect of mobile obstacles. *Biophys. J.* 52:989–997.

Saxton, M. J. 1989. The spectrin network as a barrier to lateral diffusion in erythrocytes: a percolation analysis. *Biophys. J.* 55:21–28.

Saxton, M. J. 1993. Lateral diffusion in an archipelago: single-particle diffusion. *Biophys. J.* 64:1766–1780.

Saxton, M. J. 1994. Single-particle tracking: models of directed transport. *Biophys. J.* 67:2110–2119.

Schmidt, C. E., A. F. Horwitz, D. A. Lauffenburger, and M. P. Sheetz. 1993. Integrin-cytoskeletal interactions in migrating fibroblasts are dynamic, asymmetric, and regulated. *J. Cell Biol.* 123:977–991.

Sheetz, M. P. 1983. Membrane skeletal dynamics: role in modulation of red cell deformability, mobility of transmembrane proteins, and shape. *Semin. Hematol.* 20:175–188.

Sheetz, M. P. 1993. Glycoprotein motility and dynamic domains in fluid plasma membranes. *Annu. Rev. Biophys. Biomol. Struct.* 22:417–431.

Sheetz, M. P., and E. L. Elson. 1993. Measurement of membrane glycoprotein movement by single-particle tracking. *In* Optical Microscopy: Emerging Methods and Applications. B. Herman and J. J. Lemasters, editors. Academic Press, San Diego, CA. 285–294.

Sheetz, M. P., M. Schindler, and D. E. Koppel. 1980. Lateral mobility of integral membrane proteins is increased in spherocytic erythrocytes. *Nature.* 285:510–512.

Sheetz, M. P., S. Turney, H. Qian, and E. L. Elson. 1989. Nanometre-level analysis demonstrates that lipid flow does not drive membrane glycoprotein movements. *Nature.* 340:284–288.

Svoboda, K., and S. M. Block. 1994. Biological applications of optical forces. *Annu. Rev. Biophys. Biomol. Struct.* 23:247–285.

Tsuji, A., and S. Ohnishi. 1986. Restriction of the lateral motion of band 3 in the erythrocyte membrane by the cytoskeletal network: dependence on spectrin association state. *Biochemistry.* 25:6133–6139.

Tsuji, A., K. Kawasaki, S. Ohnishi, H. Merkle, and A. Kusumi. 1988. Regulation of band 3 mobilities in erythrocyte ghost membranes by protein association and cytoskeletal meshwork. *Biochemistry.* 27: 7447–7452.

Ungewickell, E., and W. Gratzer. 1978. Self-association of human spectrin: a thermodynamic and kinetic study. *Eur. J. Biochem.* 88:379–385.

Vaz, W. L. C, and P. F. F. Almeida. 1993. Phase topology and percolation in multi-phase lipid bilayers: is the biological membrane a domain mosaic? *Curr. Opin. Struct. Biol.* 3:482–488.

Wang, Y.-l., J. D. Silverman, and L.-g. Cao. 1994. Single particle tracking of surface receptor movement during cell division. *J. Cell Biol.* 127: 963–971.

Zhang, F., B. Crise, B. Su, Y. Hou, J. K. Rose, A. Bothwell, and K. Jacobson. 1991. Lateral diffusion of membrane-spanning and glycosylphosphatidylinositol-linked proteins: toward establishing rules governing the lateral mobility of membrane proteins. *J. Cell Biol.* 115:75–84.

Zhang, F., G. M. Lee, and K. Jacobson. 1993. Protein lateral mobility as a reflection of membrane microstructure. *BioEssays.* 15:579–588.